ARTICLE
https://doi.org/10.1590/2317-488920240037

BJGEO Brazilian Journal of Geology

High- and Low-Ti tholeiites in the Eastern Parnaíba Basin: Regional correlations with Mesozoic large igneous provinces

Cícera Neysi de Almeida[1]*, Julio Cezar Mendes[1], Sérgio de Castro Valente[2], Francisco de Assis Negri[3], Alan Miranda[2], Artur Corval Vieira[2], Sílvia Regina de Medeiros[1], Leonardo Borghi[1], Pedro Miloski[4], Mayara Cardoso[5], Juliana Godot[6]

Abstract
Two tholeiitic magmatic events are recorded at the Eastern Border of the Parnaíba Basin comprising the Jurassic Mosquito Formation and the Cretaceous Sardinha Formation. They are chronocorrelated to the Central Atlantic Magmatic Province Large Igneous Province (CAMP LIP) and Equatorial Atlantic Magmatic Province (EQUAMP LIP), respectively. The latter is also chronocorrelated with the Paraná-Etendeka Province (PEMP LIP). Five groups of tholeiitic rocks are representative of magmatic episodes with different ages and tectono-magmatic context: Low-Ti Group I, High-Ti Group IIa, High-Ti Group IIb, High-Ti Group III, and High-Ti Group IV. The geochemical data of Groups I, IIa, and IIb are similar to those of tholeiitic basalts from Jurassic CAMP LIP, whereas rocks in Groups III and IV can be related to the Cretaceous EQUAMP LIP as well as High-Ti basalts of the PEMP LIP. The chemical differences between the two magmatic events indicate changes in the mantle composition underlying to the Parnaíba Basin over geological time. It is likely that the Brasiliano-Pan African orogenies, which preceded Jurassic rifting, affected the mantle sources of the Groups I and II magmas. Conversely, the composition of the mantle underlying the Parnaíba Basin was modified by the impingement of a mantle plume during the Cretaceous.

KEYWORDS: Sardinha and Mosquito Formations; continental flood basalt; deep mantle plume; Central Atlantic Magmatic Province.

1 INTRODUCTION

The Parnaíba Basin is a Paleozoic intracontinental basin located in Northeast Brazil (Fig. 1). It presents an elongated shape which parallel to the direction NNE-SSW and which the geological limits are defined by tectonic reactivations of the Neoproterozoic basement structures (Góes, 1995): Transbrasiliano Lineament (NE-SW), Picos-Santa Inês Lineament (NW-SE), and the Tocantins-Araguaia Lineament (N-S). The basement of the Parnaíba Basin is composed by lithological units of the Borborema Province and the Araguaia, Gurupi, and Rio Preto fold belts.

With an area of ca. 600,000 km^2 (Góes, 1995), the depositional history of the Parnaíba Basin spans from the Paleozoic to the Mesozoic. The basin has a sedimentary stacking of 3,500 m (Lima & Leite, 1977), reaching 5,000 m in the trough of the NE-SW rift next to the Transbrasiliano Lineament. Two tectono-magmatic events were recorded in the Parnaíba Basin: the rifting of the Pangea and the consequent opening of the Central Atlantic Ocean at the Triassic-Jurassic boundary, and the rifting of the West Gondwana and the consequent opening of the South Atlantic Ocean in the Cretaceous (Merle et al., 2011).

The Early Jurassic (ca. 200–198 Ma) and Early Cretaceous (ca. 126–130 Ma) magmatic events are represented by the Mosquito and Sardinha formations, respectively (Aguiar, 1971; Baksi & Archibald, 1997; Merle et al., 2011). These authors also consider that both formations are related to time and spatial provincialities, with the occurrence of the Sardinha Formation on the eastern border of the basin and the Mosquito Formation on the western border. Nevertheless, recent works reported ages of ca. 200 Ma in sills located at the eastern border of the basin, discarding the assumed provinciality (Rodrigues, 2014). These Jurassic ages corroborate the geophysical and geochemistry evidence for the occurrence

[1]Universidade Federal do Rio de Janeiro, Instituto de Geociências, Departamento de Geologia – Rio de Janeiro (RJ), Brazil. E-mails: neysi@geologia.ufrj.br, julio@geologia.ufrj.br, silvia@geologia.ufrj.br, lborghi@geologia.ufrj.br

[2]Universidade Federal Rural do Rio de Janeiro, Instituto de Agronomia, Departamento de Petrologia e Geotectônica – Seropédica (RJ), Brazil. E-mails: labmegufrrj@gmail.com, alanmirandageo@gmail.com, corvalgeo98@gmail.com

[3]Instituto Geológico – São Paulo (SP), Brazil. E-mail: negri.francisco@gmail.com

[4]Universidade Federal do Rio de Janeiro, Programa de Pós-Graduação em Geologia, Instituto de Geociências – Rio de Janeiro (RJ), Brazil. E-mail: miloski.geo@gmail.com

[5]Universidade Federal do Rio de Janeiro – Rio de Janeiro (RJ), Brazil. E-mail: may_cardozo2@hotmail.com

[6]Universidade Federal do Rio de Janeiro, Instituto de Geociências, Programa de Pós-Graduação em Geologia – Rio de Janeiro (RJ), Brazil. E-mail: julianagodot@hotmail.com

*Corresponding author.

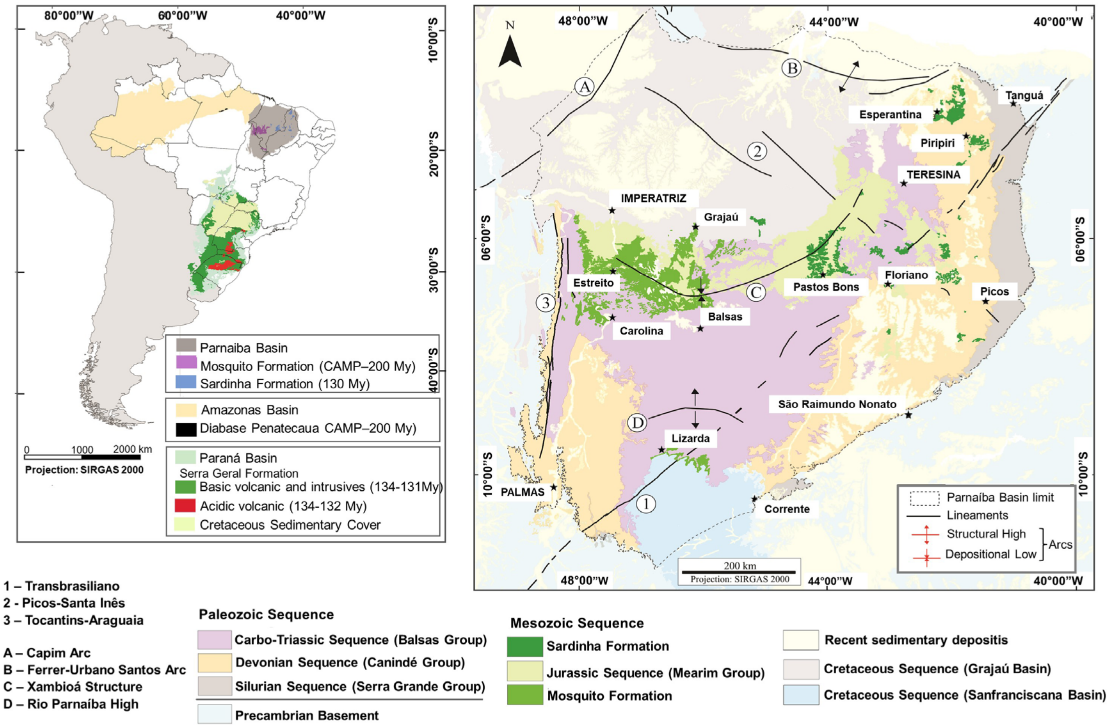

Source: Modified from Lima and Leite (1977) and Schobbenhaus et al. (2004).

Figure 1. Simplified map of the Parnaíba Basin showing the main depositional sequences and tectonic features that controlled the tectonic organization of the basin.

of Mosquito Formation, correlated to the Central Atlantic Magmatic Province (CAMP LIP) in the Eastern Border of Parnaíba Basin (EBPB), discarding the assumed provinciality (Castro et al., 2018; Macedo Filho et al., 2023a; Macedo Filho et al., 2023b).

The geodynamics of CAMP LIP is still a matter of debate, mainly regarding the participation or not of hot spots (e.g., Marzoli et al., 2018; Merle et al., 2014; Ruiz-Martínez et al., 2012). Regarding the Cretaceous event, very little has been discussed. The occurrence of tholeiitic basalt magmatic events related to different geodynamic processes within a single sedimentary basin provides a unique opportunity to investigate mantle evolution during the genesis of LIP and the fragmentation of supercontinents.

Considering the current knowledge about the EBPB magmatism, a detailed geochemical investigation is a new approach in the study related to the genesis of the basin. Therefore, the main objectives of this paper are: to provide a detailed geochemical characterization of the mafic rocks from the EBPB and to present a geochemical comparison between the magmatism of the EBPB and magmatic events associated with Jurassic Pangea breakup (CAMP LIP), as well as with Cretaceous LIPs associated to Western Gondwana breakup (EQUAMP and PEMP LIPs). Regarding the latter, geochemical characteristics could help in distinguishing between the two magmatic events, as well as highlight different compositions in the underlying mantle, the probable source of these mafic igneous occurrences. It is important to emphasize that, during the geological time elapsed between these magmatic events, the mantle may have acquired a heterogeneous character due to the resulting regional and/or local magmatic diversity.

2 GEOLOGICAL SETTING

The structural framework of the Parnaíba Basin was originated on the Jaibaras, Jaguarapi, Cococi/Rio Jucá, São Julião, and São Raimundo Nonato rifts, with ages ranging from the Neoproterozoic to the Cambrian-Ordovician (Góes et al., 1993). During the Paleozoic, the basin organization was controlled by Neoproterozoic tectonic structures (Fig. 1). The reactivation of these discontinuities as normal faults facilitated the rise of the basic magma associated with the Mosquito and Sardinha formations (Hasui & Haralyi, 1991). The stratigraphic succession of the Parnaíba Basin is predominantly siliciclastic, with subordinate evaporites and carbonate rocks, and consists of five depositional sequences: Silurian, Middle Devonian-Early Carboniferous, Late Carboniferous-Early Triassic, Jurassic, and Cretaceous sequences (Góes, 1995; Vaz et al., 2007).

Several works have been developed on the magmatic occurrence in the Parnaíba Basin and its role in hydrocarbon exploration (Thomaz Filho et al., 2008, and references therein). The main magmatic activity in the Brazilian interior sedimentary basins occurred during the Mesozoic, related to the breakup of the Gondwana Supercontinent. An important magmatic record can be seen in the Acre, Solimões, Amazonas, Parnaíba, and Paraná intracontinental basins.

Distinct basic magmatism separated by approximately 50–70 Ma occurred in the Parnaíba Basin (Bellieni et al., 1990; Baksi & Archibald, 1997), being represented by the older Mosquito Formation and the younger Sardinha Formation (Fig. 2; Aguiar, 1971, Lima & Leite, 1977). The Mosquito Formation has been reported only in the western border of the basin. It is predominantly represented by tholeiitic flood basalts and was emplaced during the opening of the Central

Atlantic Ocean (ca. 197 Ma–202 Ma, Baksi & Archibald, 1997; De Min et al., 2003; Macedo Filho et al., 2023a; Merle et al., 2011; Oliveira et al., 2018; Thomaz Filho et al., 2008). This magmatic event is part of the CAMP LIP (Marzoli et al., 1999; Marzoli et al., 2011; Merle et al., 2011). The younger, ca. 136–126 Ma Sardinha Formation, is represented by tholeiitic diabase sills and dikes that cluster in the EBPB (Baksi & Archibald, 1997; Fernandes et al., 2020; Fodor et al., 1990; Oliveira et al., 2018). The Sardinha magmatism is related to crustal rifting that occurred during the opening of the South and Equatorial Atlantic Ocean (Almeida, 1986; Milani & Thomaz Filho, 2000). This last event was included in the EQUAMP LIP (Hollanda et al., 2019).

Based on geochemical data, three different groups were proposed for rocks of the Mosquito Formation in the western Parnaíba Basin (Merle et al., 2011): Low-Ti tholeiites (TiO_2 < 1.3%), High-Ti tholeiites (TiO_2 > 2.0%), and evolved High-Ti tholeiites (TiO_2 > 3%). These authors obtained plagioclase $^{40}Ar–^{39}Ar$ ages of 199.7 ± 2.4 Ma for the High-Ti tholeiites, 197.2 ± 0.5 Ma and 198.2 ± 0.6 Ma for the evolved High-Ti tholeiites, and 198.5 ± 0.8 Ma for the Low-Ti tholeiites. Similar CAMP-related ages were obtained for microgabbros from the Batalha sill (ca. 199 Ma), the Itaueira sill (ca. 189 Ma), and the Canto do Buriti sill (ca. 177 Ma) in EBPB. These previously obtained $^{40}K–^{40}Ar$ ages (Caldasso & Hama 1978) are somehow similar to U–Pb ages in zircon (203.1 ± 2.2 Ma, Rodrigues, 2014) obtained for microgabbro from the Piripiri-Pedro II sill also located in EBPB (Fig. 2). Additionally, an $^{40}Ar–^{39}Ar$ age of 181.3 ± 1.7 Ma was obtained for low-Ti tholeiitic diabase near the city of Batalha also in eastern Parnaíba (Heilbron et al., 2018). Sardinha Formation is divided into two groups: Low- and High-Ti tholeiites (Baksi & Archibald, 1997; Bellieni et al., 1990; Fodor et al., 1990). Reported ages for the Sardinha Formation range from 129 to 134 Ma.

Ar–Ar dating in Low-Ti CAMP rocks in North Brazil (Roraima and Amazonas and sills) and in the Parnaíba Basin yielded ages ranging from 199.0 ± 2.4 to 203.3 ± 0.6 Ma and 181 ± 2 to 193 ± 2 Ma, respectively, while high-Ti Cassiporé dikes and Parnaíba Basin showed an age of 197.1 ± 1.8 Ma–199.7 ± 1.6 Ma (Fernandes et al., 2020; Macedo Filho et al., 2023b; Marzoli et al., 2011). U–Pb dating yielded the 201.6 Ma for CAMP in Guinea and Bolívia (Low-Ti basalts), and values of "201.525–201.470 Ma" (sic) and "201.470 Ma" (sic) for Low-Ti and High-Ti basalts in the Amazonas, respectively (Davies et al., 2017; Heimdal et al., 2020). These ages are similar to those obtained in the Parnaíba Basin, indicating an initial low-Ti magmatism for CAMP. However, two magmatic episodes can be depicted by the ages obtained for CAMP rocks in the Amazonas: the main CAMP, with Low-Ti overlap, and a second High-Ti phase (Heimdal et al., 2020). The geochronological data are summarized in Table 1 (https://doi.org/10.5281/zenodo.14775074).

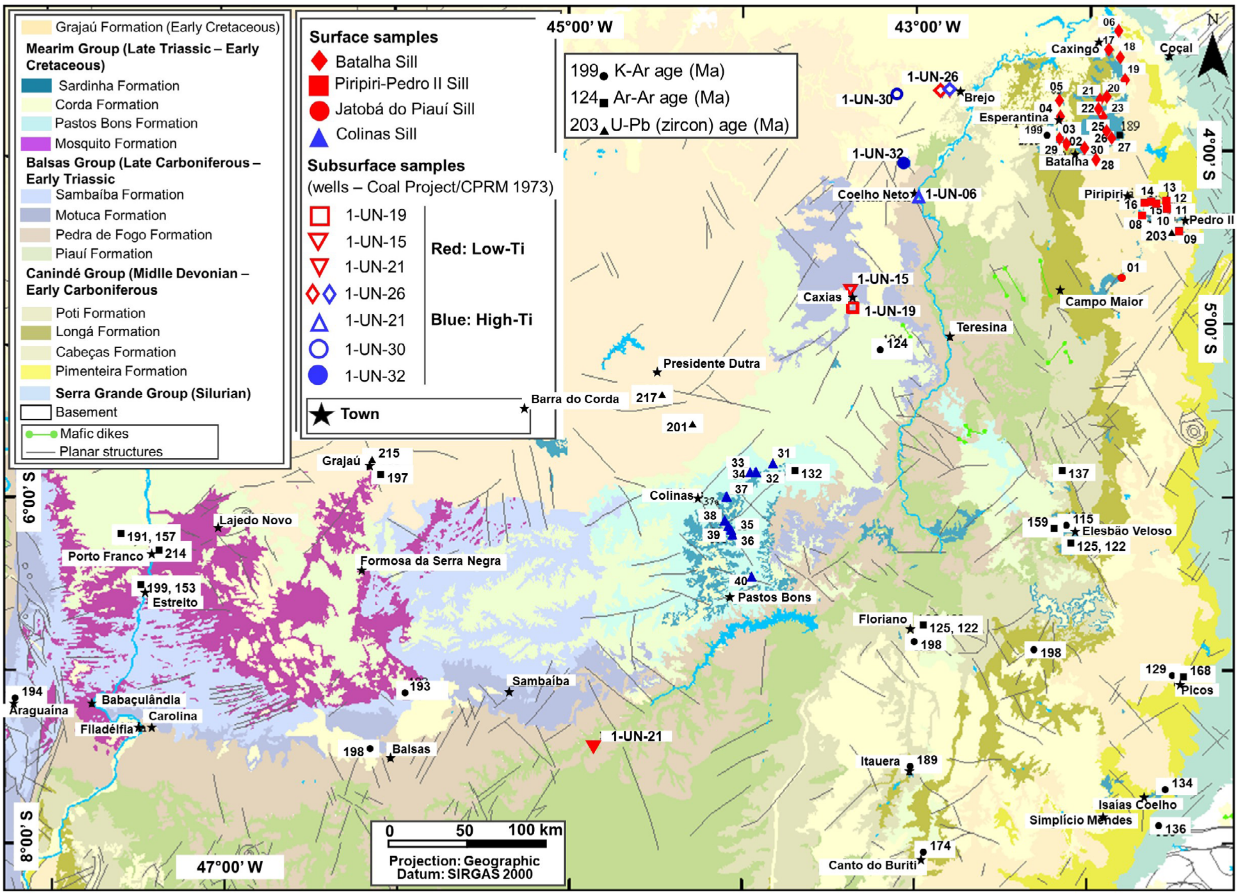

Figure 2. Simplified geological map of the eastern border of the Parnaíba Basin highlighting the sites with chemical analyses and dated samples. Modified from Lima and Leite (1977) and Schobbenhaus et al. (2004). Ages compiled from Baksi and Archibald (1997), Bellieni et al. (1990), Merle et al. (2011), Rodrigues (2014).

3 MATERIAL AND METHODS

The studied rocks were sampled from seven boreholes (1-UN-06-PI, 1-UN-15-PI, 1UN-19-PI, 1UN-21-PI, 1-UN-26-PI, 1UN-30-PI, and 1UN-32-PI) drilled in the Parnaíba Basin (Leite et al., 1975) and outcrop nearby the cities of Caxingó, Esperantina, Batalha, Piripiri and Pedro II in the Piauí State, and Colinas and Pastos Bons in the Maranhão State (Fig. 2).

A total of 86 samples were analyzed for major and trace elements, including the whole set of rare earth elements (REEs). Major and trace elements were measured by inductively coupled plasma-atomic emission spectroscopy (ICP-AES) and inductively coupled plasma-mass spectrometry (ICP-MS), respectively, in the ActLabs (Ontario, Canada) and ALS (Lima, Peru) laboratories. Each sample was reduced to powder and mixed in a flux of lithium borate, and fused in an induction furnace. The resulting glass was dissolved in a solution of nitric acid for ICP-MS analysis. For the ICP-AES analysis, the acid digestion was made by four acids: hydrofluoric, a mixture of nitric and perchloric acids, and hydrochloric acid after dryness, respectively. The detection limit for the analysed oxides was 0.01 wt%. For the selected trace elements, detection limits at ALS and ActLabs ranged from 0.05 to 5 ppm. Detection limits for the selected trace element analyses at ALS and ActLabs were 0.05–5 ppm. Accuracy was measured on the basis of international standards NIST 694, OREAS 100, and OREAS 101, whereas precision was measured by duplicating samples GP-10, GP-32, and 1UN32- 219.85. The geochemical data and geographical coordinate samples are shown in Tables 2 and 5 (https://doi.org/10.5281/zenodo.14775074).

Mineral chemistry in pyroxene and plagioclase was performed using an electron microprobe (JEOL, model JXA 8230) from the Electron Microprobe Laboratory (LABSONDA Laboratory at the Universidade Federal do Rio de Janeiro), using 5 wavelength-dispersive spectrometers (WDS) equipped with low-diffraction efficiency (LDE), lithium fluoride (LIF), thallium acid phthalate (TAP), and pentaerythritol (PET) crystal analyzers. The analytical conditions were 15 kV accelerated voltage, 20 mA probe current, 1 μm beam diameter, and ZAF correction, and the standards Plagioclase An-65 (Astimex Scientific Limited) and Cr-Augite (Smithsonian) were used to perform the quantitative analyses.

4 RESULTS

4.1 Petrography

The nomenclature of the basic rocks composed of clinopyroxene and plagioclase used in this paper is based on grain size in accordance with Gill (2010). As such, basalt is a fine-grained mafic igneous rock (< 1.0 mm) that can constitute floods with variable volume or be chilled in the margin of tabular bodies. Microgabbro comprises a medium-grained rock (1.0–3.0 mm), and gabbro is a coarse-grained one (> 3.0 mm). Based on this nomenclature, three petrographic facies were recognized in the samples investigated in this paper, as follows.

4.2 Basalt facies

This facies was identified in thin bodies (0.75–2.0 m) of the boreholes or in the edges of outcropping sills (Fig. 3a). The rock is hypocrystalline, hypidiomorphic, to xenomorphic, with a predominant glomeroporphyritic to porphyritic texture, showing phenocrysts of plagioclase, pyroxene, ± olivine immersed in a fine to very fine-grained groundmass. The groundmass exhibits subophitic, intergranular, and intersertal textures (Figs. 3b and 3c), which reflect variation in the undercooling rate.

The essential minerals are plagioclase and clinopyroxene. Accessory minerals are orthopyroxene, hornblende (replacing pyroxene), olivine, apatite, and opaque minerals. Secondary minerals include talc, serpentine, saponite iddingsite, uralite, chlorite, epidote, carbonates, and leucoxene. Plagioclase phenocrysts (0.4–1.0 mm) are prismatic, euhedral to subhedral, occurring as isolate crystals or in aggregates with pyroxene. They commonly exhibit normal zoning with compositions ranging from An_{84-63} in the cores to An_{74-47} in rims. In the groundmass, or in aphyric samples, plagioclase crystals are subhedral prismatic, being 0.2–1.0 mm in size.

Clinopyroxene is predominantly augite, with compositions varying slightly from the core ($En_{50-53}Wo_{35-38}Fs_{12-13}$) to the rims ($En_{50-52}Wo_{31-36}Fs_{12-20}$). They are subhedral prismatic crystals, smaller than 0.4 mm. In the groundmass and equigranular samples, augite also predominates but has a lower CaO content, with the composition of $En_{43-65}Wo_{29-32}$ Fs_{27-39}. In some cases, FeO_t and CaO concentrations increase from the core to rim, though the opposite is occasionally observed. Subordinate pigeonite ($En_{43-65}Wo_{8-18}Fs_{27-39}$) occurs in the matrix, as well as orthopyroxene.

Olivine is rare and observed only in subsurface samples. They are subhedral to anhedral, pseudo-hexagonal phenocrysts, up to 1.3 mm in size, and can be partially or totally altered to serpentine, talc, saponite, chlorite, and iddingsite. Opaque minerals show skeletal and granular shapes, with sizes ranging from 0.3 to 0.8 mm. Apatite is rare. A strong degree of alteration, mainly near the top of the intrusions, is remarkable in samples of the basalt facies. The minerals are replaced by secondary phases besides strong fracturing patterns, with the formation of quartz, carbonate, oxide, and uralite microveins. Hornblende occurs as the magmatic phase and deuteric alteration of clinopyroxene. According to Miloski et al. (2019), the very fine grain size, together with the presence of skeletal plagioclase, augite crystals in radial arrangement, strong fracturing and replacement by secondary phases, and fluidization, indicates that the basalt facies is a chilled margin.

4.3 Microgabbro facies

This facies is observed in the inner parts of the intrusive bodies, where grain size increases with depth (Fig. 3d). Textures include intergranular (Fig. 3e), subophitic, and seriate inequigranular varieties. Generally, the microgabbro are holocrystalline, but the glass content can reach up to 2.0 wt.%. Plagioclase and clinopyroxene are essential minerals, while orthopyroxene, olivine, hornblende replacing pyroxene,

Figure 3. (a) Chilled margin of the Piripiri-Pedro II sill in contact with the Cabeças Formation sandstone (Stop GP-07), (b) interstitial glass to skeletal plagioclase crystals forming intersertal texture in the basalt of the Piripiri-Pedro II sill chilled margin (Stop GP-07), crossed nicols, (c) intergranular texture in the basalt from the border of the well 1-UN-26-PI (66.5 m deep), (d) diabase from the Batalha sill (approximate thickness at this point 40.0 m – Stop GP-24) exposed in quarry, (e) intergranular texture in diabase showing clinopyroxene in the interstices among tabular plagioclase, crossed nicols (Stop GP-24), (f) granophyric texture in diabase of the well 1-UN-26-PI (72.8 m deep), (g) gabbro from the Batalha sill (Stop GP-21), (h) subophitic texture in the gabbro of the well 1-UN-26 (96.2 m deep), (i) granophyric texture in the gabbro of the Batalha sill (Stop GP-25).

quartz, alkali feldspar, opaque minerals, and apatite are accessory phases. Secondary minerals include kaolinite, epidote, biotite, and chlorite.

Plagioclase crystals are euhedral to subhedral prismatic, up to 4.0 mm in size, with an average of 2.5 mm. They exhibit normal zoning, with CaO contents decreasing from cores (An_{75-58}) to rims (An_{57-46}). Clinopyroxene crystals are zoned with pigeonite cores ($En_{43-67}Wo_{9-42}Fs_{23-46}$) and augite rims ($En_{22-25}Wo_{12-36}Fs_{42-63}$), though in some samples, there is an overall increase in FeO_t concentrations in augite. Orthopyroxene occurs as subhedral prismatic crystals, being 1.5 mm on average, commonly intergranular to the plagioclase. Small granular olivine crystals are disseminated in the rock. Quartz is rare, appearing as isolated crystals or in granophyric texture as aggregates up to 3.0 mm (Fig. 3f). Opaque minerals show predominantly irregular and skeletal forms and are enclosed by other minerals.

4.4 Gabbro facies

This facies occurs in outcropping sills (Fig. 3g) and borehole 1-UN-26-PI. The sill thickness in the borehole exceeds 45.0 m, as its lower contact was not drilled. The upper contact with host rock occurs at the depth of 65.83 m, and the gabbro facies occurs below the depth of 85.50 m (Miloski et al., 2019). The gabbro is a coarse, hypidiomorphic, holocrystalline rock showing intergranular, ophitic, and subophitic texture, with grain sizes between 3.5 and 5.0 mm (Fig. 3h). The mineralogy is similar to the basalt and diabase facies but with a considerable increase in modal granophyric intergrowth (Fig. 3i), reaching up to 15 wt.%. Plagioclase is tabular subhedral, up to 4.0 mm in size, poorly fractured, and altered. It presents normal zoning, marked by CaO contents decreasing from the core to rim. Augite is the predominant pyroxene. Two distinct types are identified: one with lower FeO_t and higher CaO and MgO contents, showing core compositions with $En_{29-32}Wo_{36-43}Fs_{25-34}$ and rims with $En_{23-30}Wo_{36-42}Fs_{31-40}$, and another type showing higher FeO_t and lower CaO and MgO contents, with cores with $En_{21-30}Wo_{40}Fs_{30-39}$ and rims with $En_{19-26}Wo_{33-41}Fs_{33-42}$. In both types, there is an increase in FeO_t contents at the rims of this mineral. Acicular or prismatic apatite crystals smaller than 0.5 mm occur as inclusions, mainly in plagioclase. Similar to the other facies, opaque minerals present different shapes and show exsolution textures.

4.5 Geochemistry

Rock samples plot mostly in the subalkaline basalt and basaltic andesite fields in the TAS classification diagram (Le Bas et al., 1986) and the Nb/Y vs. Zr/Ti diagram (Winchester & Floyd, 1977, Figs. 4a and 4b), except for samples from the Colinas Sill, which are transitional plotting in basalt, alkali-basalt, and trachy-andesite fields. The tholeiitic trend of the samples is demonstrated in the AFM diagram (Fig. 5).

Four rock groups can be identified in the TAS diagram (Fig. 4a): Group I is characterized by intermediate SiO_2 contents (50.1–53.4 wt.%) and Na_2O+K_2O varying between 2.5 and 3.6%, Group II is characterized by lower SiO_2 contents (42.1–49.8%) and Na_2O+K_2O ranging from 1.9 to 4 wt.%, Group III is characterized by higher SiO_2 concentrations (53–55.5%) and Na_2O+K_2O between 5.0 and 5.9%, and Group IV is characterized by samples with moderate SiO_2 contents (49.5–51.4%) and high Na_2O+K_2O (4.2–5.9%).

In the MgO vs. TiO_2 and TiO_2 vs. Fe_2O_{3t} diagrams, the proposed chemical groups are clearly separated and at least three trends can be envisaged (Figs. 6a and 6b). Group I has TiO_2 contents lower than 2.0 wt.%, delineating a trend with wide variation in MgO contents (4.0–7.7 wt.%). This group includes surface samples of the Batalha and Piripiri-Pedro II sills and subsurface samples (boreholes 1-UN-15, 1-UN-19-PI, 1-UN-21-PI, and 1-UN-26-PI). Group II presents TiO_2 contents between 2.0 and 3.0 wt.% and high MgO contents (3.4–6.7 wt.%), and the highest Fe_2O_{3t} contents when compared with the basalts of Groups III and IV. This group includes only subsurface samples (boreholes 1-UN-06-PI, 1-UN-26-PI, 1UN-30-PI, and 1UN-32-PI) and some samples of gabbro from the borehole 1-UN-26. Group III has MgO and Fe_2O_{3t} contents varying from 2.3 to 3.1 wt.% and 12.4–13.3 wt.%, respectively, including some samples of the Colinas outcrop sill. Group IV presents TiO_2 contents greater than 3.0 wt.%, also including samples from the Colinas sill. The trends of Groups I and II are characterized by a linear positive correlation between MgO and Fe_2O_{3t}, whereas Groups III and IV display a curvilinear trend, suggesting that these groups could have evolved separately.

The occurrence of Low- and High-Ti suites is typical of continental flood basalts, having been identified in several LIPS such as Paraná, Ferrar, Karoo, Deccan, and Columbia Rivers, among others (e.g., Cox et al., 1967; Mahoney et al., 2000; Peate et al., 1988). Our data point out to a Low-Ti group represented by Group I and three suites of High-Ti suites represented by Groups II, III, and IV.

Peate and Hawkesworth (1996), Peate et al. (1992), and Piccirillo et al. (1988) used Ti, Zr, Y, and Nb contents, which are high field strength elements (HFSEs) with low mobility in post-magmatic processes, to propose a chemostratigraphy for PEMP LIP basalts. It is worth mentioning that the ratios between these elements do not change during fractional crystallization (FC) process, and the same can be stated for Sr behavior in tholeiitic magmas because it is often buffered by low-pressure fractionation (Hawkesworth et al., 1992).

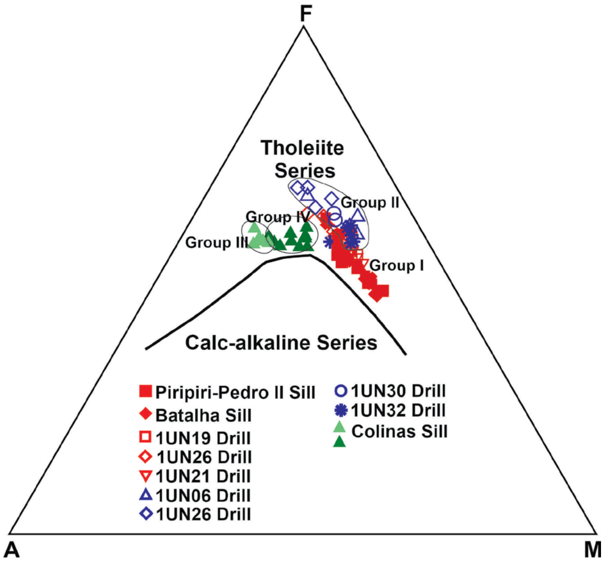

Figure 5. AFM diagram with Irvine and Baragar (1971) curve showing the tholeiitic nature of the studied rocks.

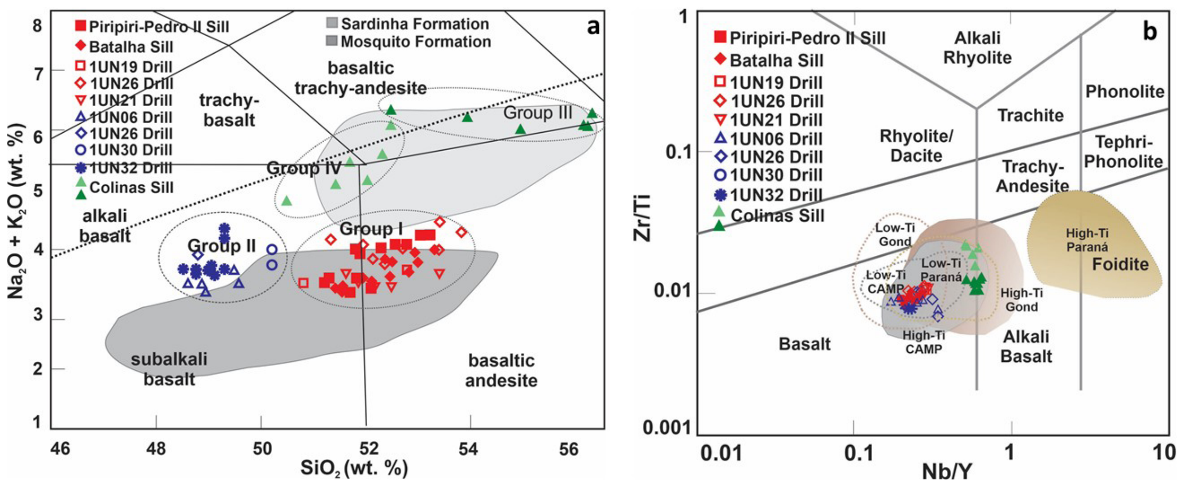

*In all figures, Paraná LIP data compiled from Machado et al., 2015, Rocha Jr. et al., 2013, Peate 1997, Peate and Hawkesworth 1996, Peate et al. 1992, 1988, Fodor et al. 1995. Southern Gondwana LIPs (Karoo/Maud Land/Vestfjella, Ferrar/Kirkpatrick) data compiled from Luttinen 2018, Luttinen et al. 2015, Whalen et al. 2015, Heinonen et al. 2010, Jourdan et al. 2007, Riley et al. 2005, Marsh et al. 1997, Fleming et al. 1997, Elliot et al. 1995, Siders and Elliot 1985. CAMP LIP data compiled from Bertrand et al. 2014, Callegaro et al. 2014, Merle et al. 2014, 2011, Marzoli et al. 2011, Deckart et al. 2005, De Min et al. 2003, Ernesto et al. 2003.

Figure 4. (a) TAS diagram with Irvine and Baragar (1971) curve showing the studied rocks are basalts, basaltic andesites and trachy-andesites. (b) ZrTi vs NbY diagram (Winchester and Floyd, 1977) with the classification of the studied rocks as sub-alkaline basalts.

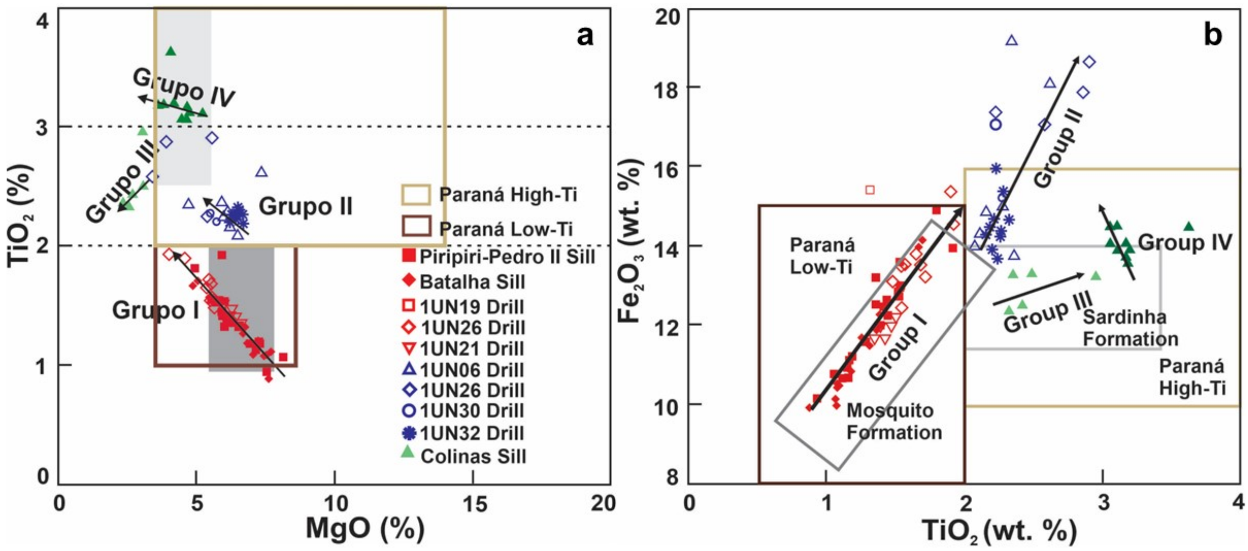

Figure 6. (a) MgO vs. TiO2 and (b) TiO2 vs. Fe2O3t diagrams with the separation of the chemical groups and proposition of three different trends.

Following such a geochemical approach, Sr and some ratios between these HFSE have been used to classify basalts into several High- and Low Ti suites in PEMP LIP (Esmeralda, Gramado, Ribeira, Paranapanema, Pitanga, and Ubirici, e.g., Peate & Hawkesworth, 1996).

Considering the time correspondence of the basalts from EBPB with either CAMP or PEMP LIPs (Baksi & Archibald, 1997; Rodrigues, 2014), that Sr variations were not affected by the FC of plagioclase, we used Sr and Ti/Y, Zr/Y, and Ti/Zr ratios to separate and compare the chemical groups in basic rocks.

The Low-Ti Group I basalts have Ti/Y ratios > 250 (273–411), Ti/Zr ratios > 65 (69–101), and Sr contents mainly < 300 ppm (176–307 ppm), plotting within the Low-Ti CAMP LIP field (Figs. 7a–7c). The High-Ti Group II basalts have the highest Ti/Y ratios (359–573), Ti/Zr ratios (74–117), intermediate Zr/Y ratios (4.1–5.3), and low Sr contents (181–352 ppm). Most samples from this group plot within the High-Ti/Low-Ti CAMP LIP (Figs. 7a–7c). High-Ti Group III basalts have the lowest Ti/Y and Ti/Zr ratios (236–329 and 33–38, respectively) and high Sr contents (518–552 ppm). The High-Ti Group IV shows the highest Ti/Y ratios (397–523), low Ti/Zr ratios (61–75), and high Sr contents (477–513 ppm). The Zr/Y ratio is high in both groups (6.4–7.5), and samples plot mainly in High-Ti EQUAMP and Paraná LIPs (Figs. 7a–7c, Table 3, https://doi.org/10.5281/zenodo.14775074).

The observed geochemical characteristics suggest that all rocks of the NE and SE portions of the Parnaíba Basin (Groups I and II) should be associated with the Jurassic magmatic event (CAMP LIP) belonging to the Mosquito Formation. The rocks of Groups III and IV overlapping the Sardinha Formation field TAS diagram (Fig. 4a) are more similar to the EQUAMP and Paraná LIPs and must be associated with the Cretaceous magmatic event, belonging to the Sardinha Formation. The contrasting behavior between rocks of the same group can be attributed to different stages in magmatic processes, the degree of partial melting, or even derivation from different mantle sources.

The primitive normalized mantle (McDonough & Sun, 1995) and REE chondrite-normalized (Boynton, 1984) diagrams of the EBPB basic rocks, despite the enrichment for all incompatible elements, show different patterns (Figs. 8a and 8b).

Group I exhibits a moderately fractionated pattern (average large-ion lithophile element ($LILE_N$)/$HFSE_N$ ratio = 6.4) with strong negative Ta-Nb and positive Pb anomalies. The REE chondrite-normalized diagram displays a slightly fractionated pattern (La_N/Yb_N = 1.1–2.6) and absence or weak negative Eu anomaly (Eu* = 0.85–0.9), that, coupled with no evident Sr trough, suggests an absence of plagioclase fractionation.

A different behavior is depicted in Group II. High-Ti samples of the borehole 1-UN-26-PI show patterns similar to Group I, distinguished by the greatest enrichment in all incompatible elements and Sr trough. The REE chondrite-normalized pattern is similar to Group I. The High-Ti rocks of the other boreholes show flat patterns (average $LILE_N$/$HFSE_N$ ratio = 1.2) and little LILE enrichment, without Nb-Ta and Pb anomalies. The REE chondrite-normalized diagram is fractionated (La_N/Yb_N = 2.0–3.4), with lower light rare earth element (LREE) contents than Group I and part of Group II without or with a weak negative Eu anomaly (Eu* = 0.74–0.87). Due to this distinct behavior, High-Ti 1-UN-26-PI rocks will be designated as Group IIb and another grouping as Group IIa.

The rocks in Groups III and IV are the most enriched in incompatible elements, showing a homogeneous pattern. They present Nb-, Sr-, and Ti-negative anomalies and Rb-Ba and La-Ce spikes, with the absence of Pb anomaly. The REE chondrite-normalized diagrams are similar, strongly fractionated (La_N/Yb_N = 8.5, 18.5), showing weak negative Eu anomaly (Eu* = 0.85). Group III basalts are slightly more enriched in all incompatible elements. Despite variations among the groups, the patterns for Groups I, IIa, III, and IV show similarities to other continental flood basalts.

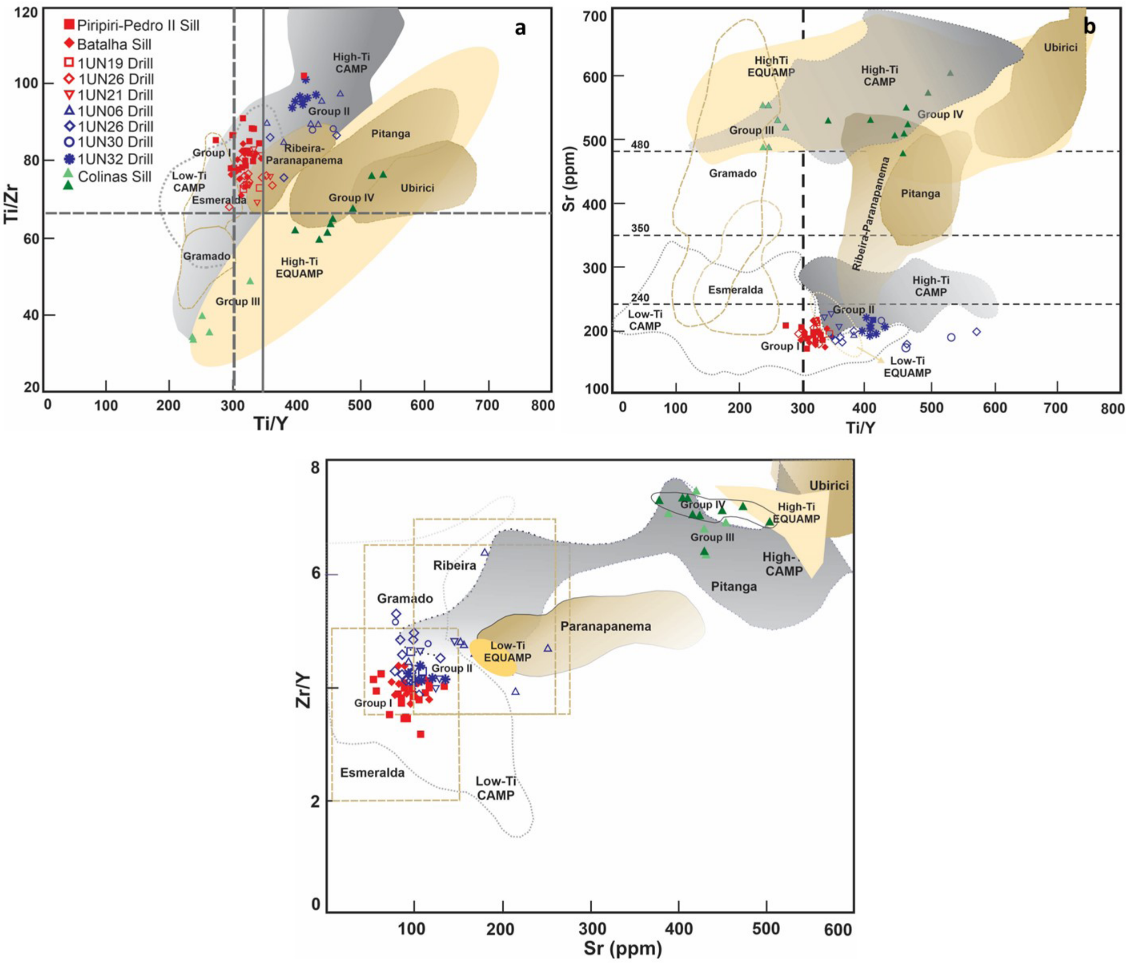

Figure 7. (a) Ti/Y vs Ti/Zr and (b) Ti/Y vs Sr and diagrams (Peate et al. 1992, Peate and Hawkesworth 1996) and (c) Sr vs Zr/Y diagram (Peate et al. 1992, Peate and Hawkesworth 1996)). All figures show the studied basic rocks and fields for the Low-Ti Paraná LIP (Gramado, Esmeralda and Ribeira) and High-Ti Paraná LIP (Paranpanema, Pitanga, Ubirici suites), CAMP and EQUAMP LIPs.

5 DISCUSSION

5.1 Geochemical comparison of mafic rocks from the Eastern Border of the Parnaíba Basin with other LIPs (Southern Gondwana and Paraná)

Taking into account the Ti/Y, Ti/Zr, Zr/Y ratios and low Sr contents (Figs. 7a–7c), the Low- and High-Ti rocks of the Groups I, IIa, and IIb (Sr < 352 ppm, LOI < 2.0) should be geochemically correlated to Jurassic CAMP LIP. The samples from Groups III and IV (Colinas sill) with the highest levels of TiO_2 tend to a greater enrichment in Sr, which could be explained by the non-crystallization of plagioclase at low pressure. However, in low SiO_2 magmas, plagioclase can crystallize before clinopyroxene at low pressure, reducing the CaO content in the magma (Callegaro et al., 2014; Ragland, 1989). The increase in Sr contents in tholeiitic basalts is often the result of the hydrothermal alteration or an abrupt assimilation event by carbonatitic rocks, marked by positive SiO_2 and negative CaO trends without marked MgO variation (Callegaro et al., 2014; Callegaro et al., 2017). However, the low LOI values in these rocks (LOI < 2.5) do not indicate alteration.

Similar behavior can be seen in the primitive mantle normalized multi-element diagrams (Figs. 8c and 8d). Groups I, IIa, and IIb (Mosquito Formation) overlap the envelope of the Low-Ti CAMP LIP in this diagram, marked by an enrichment in all incompatible elements and prominent negative Ta-Nb and positive Pb anomalies, typical features of the CAMP LIP (Callegaro et al., 2014; Merle et al., 2011). Groups III and IV (Sardinha Formation) overlap the High-Ti PEMP and EQUAMP LIPs fields, marked by higher contents in incompatible elements, with more enrichment in LILE and LREE, highlighted by Rb-Ba, La-Ce, and Nd spikes and Ta-Nb and Ti troughs. All these geochemical constraints suggest different genesis and evolution for the groups on the EBPB and in consonance with their associations to LIPs generated at different geological times.

5.2 Sources and mantle heterogeneities

Group I Low-Ti rocks from the EBPB are tholeiitic basalt to basaltic andesite, showing the highest MgO, lowest Fe_2O_{3t} and TiO_2 contents, moderate SiO_2, as well as moderate Ti/Zr, Ti/Y, Zr/Y ratios. They present low LILE and LREE and high HFSE and HREE concentrations in relation to Groups II, III, and IV, and commonly show Pb-positive and Nb-negative

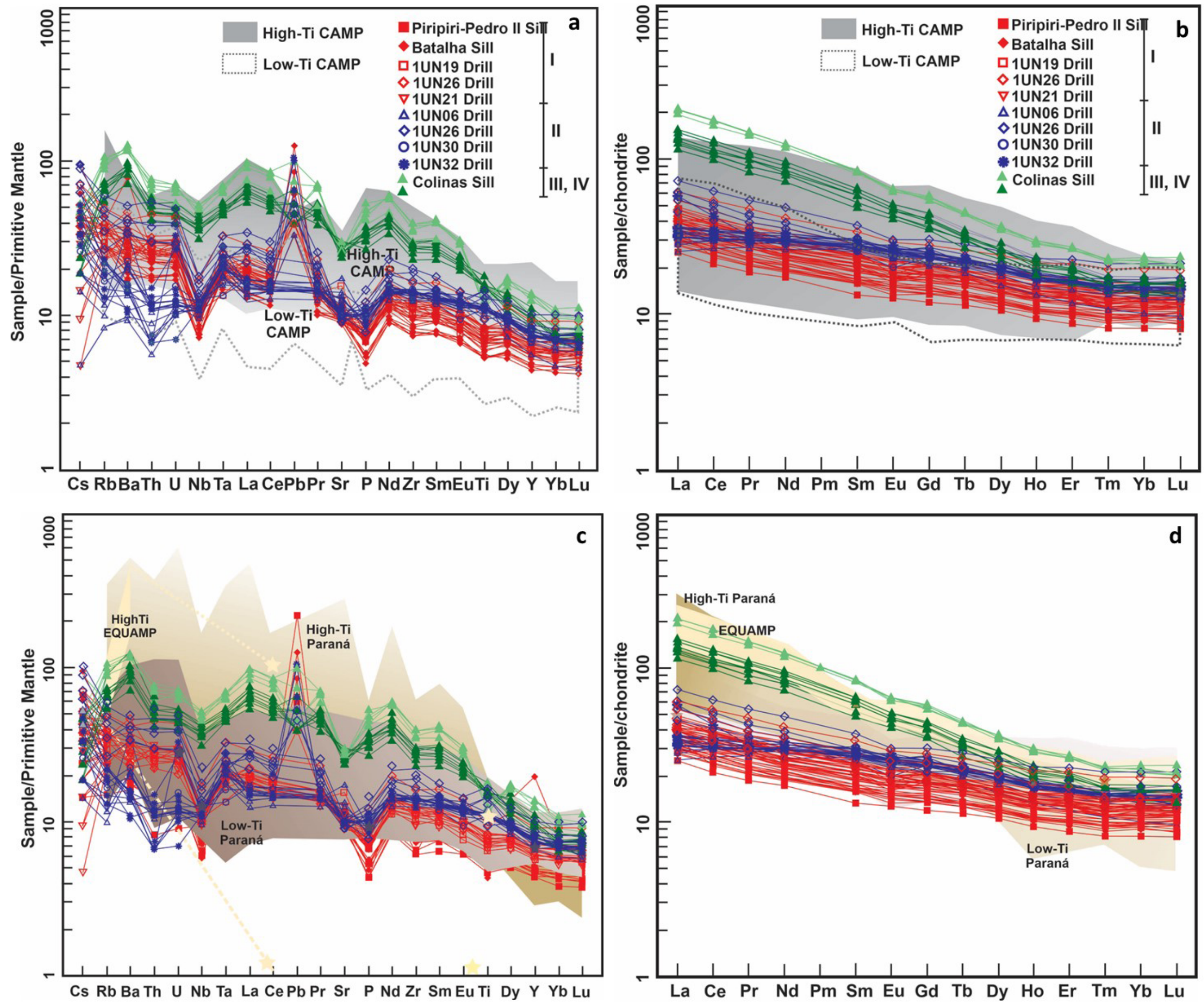

Figure 8. (a) Primitive mantle-normalized pattern (McDonough and Sun 1995) for the mafic rocks under study and Low-Ti/High-Ti CAMP fields. (b) Chondrite-normalized REE pattern (Boynton 1984) for the mafic rocks under study with Low-Ti/High-Ti CAMP fields. (c) Primitive mantle-normalized pattern (McDonough and Sun 1995) for the mafic rocks under study with Low-Ti/High-Ti Paraná and EQUAMP LIPs fields. (d) Chondrite-normalized REE pattern (Boynton 1984) for the mafic rocks under study with Low-Ti/High-Ti Paraná and EQUAMP LIPs fields.

anomalies. They have similarities mainly with the Low-Ti Jurassic CAMP LIP.

These characteristics are similar to the subcontinental lithospheric mantle (SCLM, Anderson, 1983) that can be refertilized due to metassomatic processes introducing incompatible elements, being thus taken as a source for tholeiitic continental Low-Ti basalts (e.g., Hawkesworth et al., 1992; Hergt et al., 1991). Some characteristics of tholeiitic continental basalt such as the Ta-Nb-negative anomalies and a Pb-positive anomaly have been attributed to metasomatism of the lithospheric mantle by subduction (Ivanov et al., 2008; Marsh, 1987), crustal contamination, or post-magmatic alteration (Callegaro et al., 2014; Riley et al., 2005).

Several mantle reservoirs with a substantial SCLM component have been proposed as a source of the CAMP LIP:

- SCLM metasomatized during subduction+asthenosphere (Marzoli et al., 2011; Merle et al., 2011; Riley et al., 2005)+crustal contamination (Luttinen et al., 2015);
- SCLM modified by sediment incorporation during subduction (Whalen et al., 2015), with a maximum of 10% crustal assimilation (Callegaro et al., 2014; Marzoli et al., 2018);
- mixing of asthenosphere with small volumes (1–3%) of highly enriched lamproitic melts derived from the SCLM (Callegaro et al., 2017);
- some authors consider that liquids derived only from an enriched asthenosphere mixed with sedimentary material during a previous subduction event, or modified by assimilation and fractional crystallization (AFC) or crustal contamination, can be considered as potential sources of Low-Ti CAMP (Merle et al., 2014; Riley et al., 2005).

Geochemical modeling of incompatible trace elements (La, Eu, Yb, Zr, and Nb) indicates that FC and AFC could explain the compositional variations recorded in single bodies of the same borehole and different sills (Magalhães, 2019; Miloski et al., 2019; Scribelk, 2019; Silva et al., 2017), (Table 4, https://doi.org/10.5281/zenodo.14775074). However, some issues must be highlighted. With regard to Group I, geochemical modeling points out that:

- igneous body in this group not evolved together by FC or AFC;

- the 1-UN-21 borehole is about 400 km from the other igneous bodies in this group. In turn, isotopic compositions indicate a metasomatized SCLM with asthenosphere contributions as sources for the different bodies of the 1UN-21 (Costa, 2019);
- heterogeneities in SCLM are the source of Low- and High-Ti rocks of the borehole 1-UN-26 (Miloski et al., 2019).

In relation to Groups II, III, and IV, further discussions will be carried out in the following section.

Geochemical modeling for Group II shows that compositional variation in 1-UN-06 intrusion could be explained by FC. However, similar MgO contents with different La/Yb ratios preclude FC and AFC as possible processes for the 1-UN-32 body. Notably, 40–45% of upper continental crust contamination could explain the enrichment observed in the Colinas sill rocks (Scribelk, 2019).

Geochemical modeling, low Sr, and LOI contents of the Group I basalts are not in accordance with crustal contamination or alteration. Enrichment in LILE, LREE, and Ta-Nb-negative anomalies and prominent positive Pb anomaly support a refertilized SCLM as a source of the parental magmas of Group I, while crustal contamination or another source could have played an important role in the magma origin of Groups II, III, and IV.

The TiO_2/Yb vs. Th/Nb diagram (Pearce et al., 2021) divides LIP basalt into three types (Fig. 9). In this diagram, Group I rocks are classified as type II LIP, with a source dominated by the subduction-modified lithospheric mantle, i.e., refertilized lithosphere by previous events of subduction. Group I overlaps the envelope of the Jurassic and Cretaceous Low-Ti LIPs, giving a diagonal positive trend with a narrow dispersion of TiO_2/Yb and Th/Nb. This, coupled with the lowest Ti/Y and Ti/Zr and high Zr/Y, indicates the melting of the shallow

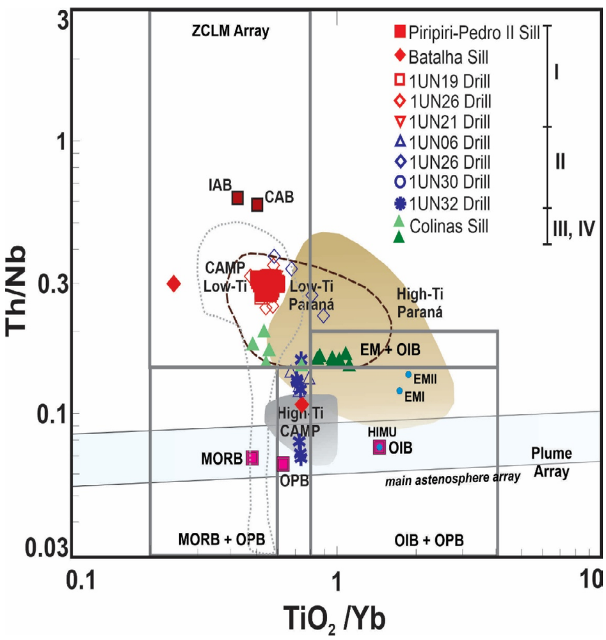

Figure 9. TiO_2/Tb vs Th/Nb (Pearce et al., 2021) showing the LIP printing classification for the Groups I, IIa, IIb, III and IV from the EBPB with Low-Ti/High-Ti CAMP, and Paraná LIPs fields.

mantle enriched by the subduction process with low residual garnet (Pearce, 1982; Pearce et al., 2021).

Group IIa comprises tholeiitic basalts with moderate MgO, Fe_2O_{3t}, and TiO_2 contents, characteristics ascribed to asthenosphere-derived magmas (Harte, 1983). Normalized spidergrams, similar to E-MORB (Hémond et al., 2006), corroborate the participation of an asthenospheric source in the genesis of these rocks. At the same time, a moderate or absent Nb anomaly, moderate negative Ti and positive Pb anomalies, and high Ti/Zr, Ti/Y, and moderate Zr/Y anomalies suggest that the source of these rocks is the result of mixing between depleted and enriched source components.

In the TiO_2/Yb vs. Th/Nb diagram, samples of Group IIa show greater similarities with type IIIa LIP plotting mostly into the high-Ti CAMP LIP fields, intermediate to the MORB+OPB and OIB+OPB plume segments developing a vertical trend, that requires asthenosphere participation and little interaction with SCLM refertilized by subduction or crustal contamination. Multi-elemental patterns showing the lowest enrichment and insertion below the SZLM segment (subduction-modified lithospheric mantle) imply no crustal contamination, although the Th/Nb vertical dispersion supports variable degrees of interaction with subduction-modified components. Spinel-peridotite melting is demonstrated by the low and constant TiO_2/Yb (Pearce et al., 2021). Similar sources were suggested for CAMP High-Ti rocks (Deckart et al., 2005; Marzoli et al., 2011; Marzoli et al., 2018; Merle et al., 2011).

Group IIb also comprises tholeiitic basalts with lower MgO contents and higher Fe_2O_{3t}, TiO_2, LILE, HFSE, LREE, and HREE concentrations, compared to Groups I and IIa. Group IIb is classified as Type IIIb LIP displaying a diagonal trend between EM+OIB and SZLM segment (subduction-modified lithospheric mantle), demonstrating an interaction between the enriched asthenosphere and the crustal component (Pearce et al., 2021). Since AFC has been ruled out by geochemical modeling, the enriched characteristics in this group were attributed to vertical mantle variation by subduction components (Miloski et al., 2019). Moderate dispersion TiO_2/Yb ratios also point to a variation at the melting depth.

Group III and IV basalts have the lowest MgO, highest TiO_2, and moderate FeO observed among all the groups, which could indicate the participation of a crustal component in the genesis of the parental magma, as suggested by Piccirillo and Cox (1988). However, a fertile asthenospheric mantle is rich in Fe-Ti, the basaltic components, and depleted in Mg and Cr (Harte, 1983). The lowest Ti/Y and Ti/Zr preclude enriched sources, corroborating contributions from asthenosphere sources; nevertheless, the highest enrichment in LILE, LREE, Zr/Y, along with geochemical modeling, indicates the participation of crustal contamination. The apparently contrasting chemical characteristics recorded in Groups III and IV may reflect multicomponent sources.

Group III is classified as type IIIa LIP at the MORB-OPB/SZLM boundary (Pearce et al., 2021), showing low TiO_2/Yb with moderate dispersion. These characteristics favor the interaction between asthenosphere, modified by a plume component, and refertilization of the lithospheric mantle by subduction

(Pearce et al., 2021). Group IV has the highest Ti/Y and Zr/Y, which, coupled with the high enrichment in incompatible elements and Ti/Zr, also suggests similar ocean island basalt (OIB) sources (Pearce & Norry, 1979). It is classified as Type IIIb LIP (Pearce et al., 2021), plotting into the EM+OIB segment, consonant to HFSE ratios. The Th/Nb small-range and the wide dispersion TiO_2/Yb ratios at high Nb/Y of Group IV reinforce a plume contribution to the source and melting depths with more residual garnet. The samples of both groups overlap the High-Ti PEMP LIP field and Sardinha Formation rocks. The distinct compositions of the EBPB basalts, reflecting source diversities, demonstrate that the mantle underlying the Parnaíba Basin changed in a relatively short period of time (ca. 70 Ma).

5.5 Geodynamic scenarios

The singular geographic distribution of the Mosquito Formation in the eastern and western borders of the Parnaíba Basin and Sardinha Formation, aligned in a belt in the center-eastern portion of the basin, along with different geochemical characteristics in the magmatic events, suggests a change in mantle geodynamics through geological time.

Several mechanisms have been proposed to explain the fragmentation of the Pangea and subsequent generation of CAMP LIP, to which Groups I, IIa, and IIb belong: thermal insulation of the lithosphere by plume impinging (Coltice et al., 2007), lithospheric delamination (Lustrino, 2005), cratonic edge-convection (Deckart et al., 2005; King & Anderson, 1995; McHone, 2000), and plume models (e.g., Ruiz-Martínez et al., 2013).

The lithogeochemical characteristics of the CAMP LIP-associated rocks on the east and west edges of the Parnaíba Basin do not indicate mantle plume participation, supporting edge-driven convection as the mechanism for lithosphere weakening and magma generation. However, it has been shown that the action of plumes and convection currents has limited effects since it protects the lithosphere from tectonic attacks (Wang et al., 2015). Geophysical data show thinning from the center to the eastern and western flanks of the Parnaíba Basin, for about 48–37 km (Daly et al., 2014). Thus, convection in a lithosphere previously modified by metasomatism during a subduction event could have been an important agent in the Jurassic geodynamics. Subduction events promoting chemical modification in the mantle underlying the Parnaíba Basin can be associated with previous stages of the Brasiliano/Pan-African collisions that gave rise to the orogens bordering the basin.

With regard to the Sardinha Formation, its alignment, together with its geochemical characteristics, points to the participation of a deep mantle plume in promoting heat and as a source of Cretaceous magmatism. Geochemical modeling and isotopic compositions discard a deep mantle plume participation in PEMP and CAMP LIPs (Peate & Hawkesworth, 1996; Rocha-Junior et al., 2013, and references therein); however, the participation of a deep mantle plume in PEMP LIP is still an open debate. The isotopic compositional variation in the PEMP LIP is attributed to the change in the Tristan-Gough plume composition over time, due to horizontal displacement plates that generated a bilaterally zoned plume (Hoernle et al., 2015). Activation of this plume is seen as one of the models for the South Atlantic Ocean rifting (Cordani et al., 1980). Our data suggest a complex scenario for the origin of Groups III and IV, where different sources and mechanisms (tectonics and plumes) could have acted together.

Hollanda et al. (2019) correlated giant dike swarms, in the Borborema Province, with similar ages and compositions but different trends (E-W, NE-SW, and NW-SE), to the Sardinha Formation, defining the EQUAMP LIP. These dikes are coeval to the tholeiitic dike swarm of the Benue Trough, which is the triple junction point associated with the Atlantic Ocean opening. Radial dike systems are important evidence of the existence of plumes (McHone, 2000) and coupled with the geochemical data reinforce the hypothesis of the impingement of a mantle plume in the Cretaceous underlying mantle of the Parnaíba Basin.

6 CONCLUSIONS

The evaluation of the geochemical data presented herein indicates the difficulty in inserting continental basaltic provinces, or at least part of them, in a single-generation model. It is also noted that the different continental flood basalt (CFB) provinces have many similarities resulting from "common sources" for Low- and High-Ti basalts, and that the geochemical parameters used by some authors to distinguish these suites apply only to the province in which the parameters were established. The role of tectonic features, shaping physical and chemical characteristics, and further particularities among the various provinces, should also be taken into account.

In spite of that, the geochemical data for the EBPB basic rocks enable the distinction of five groups related to different signatures, imprinted mainly due to changes in the mantle over time: Jurassic Low-Ti Group I (SZLM––lithospheric mantle modified by subduction), Jurassic High-Ti Group IIa (interaction between depleted asthenosphere and SZLM), Jurassic High-Ti Group IIb (interaction between subduction-enriched asthenosphere and SZLM), and Cretaceous High-Ti Groups III and IV (different degrees of interaction between plume-enriched asthenosphere and SZLM).

Taking into account the possibility that Low-Ti basalts of the CAMP LIP are younger (e.g., Heimdal et al., 2020), the generation of magmas started in shallow SZLM, followed by melting of deeper sources, depleted and enriched asthenosphere. Furthermore, the data also enabled geochemical correlations between those five groups to magmatic events, pointing out that the low-Ti rocks were observed in the Batalha and Piripiri-Pedro II sills, as well as the low-Ti and high-Ti subsurface rocks in their surroundings. They present characteristics more compatible with Jurassic CAMP LIP instead of the geographical provinciality that considers the EBPB magmatism as representing a Cretaceous event. Moreover, the dating presented by Heilbron et al. (2018) and Rodrigues (2014), showing Jurassic ages for the Batalha and Piripiri-Pedro II sills and geophysical data (Mocitaiba et al., 2017), indicate that the Mosquito Formation is not restricted to the western border of the Parnaíba Basin, occurring intensely on all edges, while Cretaceous rocks dominate the east-central portion.

ACKNOWLEDGMENTS

The authors acknowledge the sponsor of Geopark Oil and Gas and the strategic importance of ANP (National Petroleum Agency) support, through the P&D obligatory regulation (technical collaboration no. 19.343). The authors would like to thank the reviewers, Dr. Anderson da Costa Santos and Dr. Fábio Braz Machado, for their valuable suggestions that improved the paper. We would like to express our very special thanks to Dr. Sara Callegaro for her careful prior review of the paper, whose recommendations were fundamental in the preparation of the paper presented here.

ARTICLE INFORMATION

Manuscript ID: 20240037. Received on: 13 NOV. 2024. Approved on: 31 MAR 2025.

How to cite: Almeida, C. N., Mendes, J. C., Valente, S. C., Negri, F. A., Miranda, A. W., Corval, A., Medeiros, S. R., Borghi, L., Miloski, P., Cardoso, M., & Godot, J. (2025). High- and Low-Ti tholeiites in the Eastern Parnaíba Basin: Regional correlations with Mesozoic large igneous provinces. *Brazilian Journal of Geology*, *55*, e20240037. https://doi.org/10.1590/2317-488920240037

CNA: Project administration, Data collection, Data analysis and interpretation, Development of hypotheses and models, Manuscript preparation. JCM: Data analysis and interpretation, Development of hypotheses and models, Manuscript preparation. SCV: Data collection, Data analysis and interpretation, Development of hypotheses and models, Manuscript preparation. FAN: Data collection, Manuscript preparation. AWM: Data collection, Data analysis and interpretation, Development of hypotheses and models. AC: Data analysis and interpretation, Development of hypotheses and models. SRM: Data collection, Data analysis and interpretation, Development of hypotheses and models, Project administration, Acquisition of financial resources, Manuscript preparation. Leonardo Borghi: Project administration, Acquisition of financial resources, Manuscript preparation. PM: Data analysis and interpretation, Development of hypotheses and models. MC: Data analysis and interpretation, Development of hypotheses and models. JG: Data analysis and interpretation, Development of hypotheses and models.

Data availability statement: The datasets generated and/or analyzed during the current study are publicly available at https://doi.org/10.5281/zenodo.14775074

Competing interests: The authors declare no competing interests.

SCIENTIFIC EDITOR: Carlos Grohmann
ASSOCIATE EDITOR: Andres Folguera

REFERENCES

Aguiar, G. A. (1971). Revisão geológica da bacia paleozóica do Maranhão. In: 25° Congresso Brasileiro de Geologia, 3, 113-122.

Almeida, F. F. M. (1986). Distribuição regional e relações tectônicas do magmatismo pós- paleozoico no Brasil. *Revista Brasileira de Geociências, 16*(4), 325-349.

Anderson, D. L. (1983). Chemical composition of the mantle. Proceedings of fourteenth lunar and planetary science conference, Part 1. *Journal of Geophysics Research, 88*(Suppl. 1), B41-B52. https://doi.org/10.1029/JB088iS01p00B41

Baksi, A. K., & Archibald, D. A. (1997). Mesozoic igneous activity in the Maranhão province, northern Brazil: ^{40}Ar/ ^{39}Ar evidence for separate episodes of basaltic magmatism. *Earth and Planetary Science Letters, 15*(3-4), 139-153. https://doi.org/10.1016/S0012-821X(97)81844-4

Bellieni, G., Macedo, M. H. F., Petrini, R., Picirillo, E. M., Cavazzini, G., Comin-Chiaramonti, P., Ernesto, M., Macedo, J. W. P., Martins, G., Melfi, A. J., Pacca I. G., & De Min, J. (1990). Evidence of magmatic activity related to Middle Jurassic to early cretaceous rifting from northeastern Brazil (Ceará-Mirim): K/Ar age, paleomagnetism, petrology and Sr-Nd isotope characteristics. *Chemical Geology, 97*(1-2), 9-32. https://doi.org/10.1016/0009-2541(92)90133-P

Bertrand, H., Fornari, M., Marzoli, A., Garcia-Duarte, R., & Sempere, T. (2014). The Central Atlantic Magmatic Province extends into Bolivia. *Lithos*, *188*, 33-43. https://doi.org/10.1016/j.lithos.2013.10.019

Boynton, W. V. (1984). Geochemistry of rare earth elements: meteorite studies. In P. Henderson (Ed.), *Rare earth element geochemistry* (pp. 63-114). Elsevier.

Caldasso, A. L. S., & Hama, M. (1978). Posicionamento estratigráfico das rochas básicas da Bacia do Parnaíba. In XXX Congresso Brasileiro de Geologia, 2, 567-581.

Callegaro, S., Marzoli, A., Bertrand, H., Blichert-Toft, J., Reisberg, L., Cavazinni, G., Jourdan, F., Davies, J. H. F. L., Parisio, L., Bouchet, R., Paul A., Schalteer, U., & Chiaradia, M. (2017). Geochemical constraints provided by the freetown layered Complex (Sierra Leone) on the origin of high-ti tholeiitic CAMP magmas. *Journal of Petrology*, *58*(9), 1811-1840. https://doi.org/10.1093/petrology/egx073

Callegaro, S., Rapaille, C., Marzoli, A., Bertrand H., Chiaradia, M., Reiberg, L., Bellieni, J., Martins, L., Madeira, J., Mata, J., Youbi, N., De Min, A., Azevedo, M. R., & Bensalah, M. K. (2014). Enriched mantle source for the Central Atlantic magmatic province: New supporting evidence from southwestern Europe. *Lithos*, *188*, 15-32. https://doi.org/10.1016/j.lithos.2013.10.021

Castro, D. L., Oliveira, D. C., & Hollanda, M. H. B. M. (2018). Geostatistical interplay between geophysical and geochemical data: mapping litho-structural assemblages of mesozoic igneous activities in the Parnaíba Basin (NE Brazil). *Surveys in Geophysics*, *39*, 683-713. https://doi.org/10.1007/s10712-018-9463-5

Coltice, N., Phillips, B. R., Bertrand, H., Ricard, Y., & Rey, P. (2007). Global warming of the mantle at the origin of flood basalts over supercontinents. *Geology*, *35*(5), 391-394. https://doi.org/10.1130/G23240A.1

Cordani, U. G., Sartori, P. L. P., & Kawashita, K. (1980). Geoquímica dos isótopos de estrôncio e a evolução da atividade vulcânica na Bacia do Paraná (Sul do Brasil) durante o Cretáceo. *Anais da Academia Brasielira de Ciências*, *52*(4), 811-818.

Costa, J. P. S. (2019). *Caracterização petrográfica e geoquímica das rochas ígneas presentes no Poço 1-UN-21-PI, Riacho da Volta, município de Uruçuí, PI* [Dissertation, Universidade Federal do Rio de Janeiro].

Cox, K. G., Macdonald, R., & Hornung, G. (1967). Geochemical and petrographic provinces in the Karoo basalts of southern Africa. *American Mineralogy*, *52*(9-10), 1451-1474.

Daly, M. C., Andrade, V., Barousse, C. A., Costa, R., McDowell, K., Piggott, N., & Poole, A. J. (2014). Brasiliano crustal structure and the tectonic setting of the Parnaíba basin of NE Brazil: Results of a deep seismic reflection profile. *Tectonics*, *33*(11), 2102-2120. https://doi.org/10.1002/2014TC003632

Davies, H. F. L., Marzoli, A., Bertrand, H., Youbi, N., & Schatelgger, U. (2017). End-Triassic mass extinction started by intrusive CAMP activity. *Nature Communications*, *8*, 15596. https://doi.org/10.1038/ncomms15596

Deckart, K., Bertrand, H., & Liegeois, J. P. (2005). Geochemistry and Sr, Nd, Pb isotopic composition of the Central Atlantic Magmatic Province (CAMP) in Guyana and Guinea. *Lithos*, *82*(3-4), 289-314. https://doi.org/10.1016/j.lithos.2004.09.023

De Min, A., Piccirillo, E. M., Marzoli, A., Bellieni, G., Renne, P. R., Ernesto, M., & Marques, L. S. (2003). The Central Atlantic Magmatic Province (CAMP) in Brazil: petrology, geochemistry, $^{40}Ar/^{39}Ar$ ages, paleomagnetism and geodynamic implications. In W. E. Hames, G. McHone, P. R. Renne & C. Ruppert (Eds.), *The Central Atlantic Magmatic province: insights from fragments of Pangea* (pp. 91-128). American Geophysical Union.

Ernesto, M., Bellieni, G., Piccirillo, E. M., Marques, L. S., De Min, A., Pacca, I. G., Martins, G., & Macedo, J. W. P. (2003). Paleomagnetic and geochemical constraints on the timing and duration of the CAMP activity in Northeastern Brazil. In W. E. Hames, G. McHone, P. R. Renne & C. Ruppert (Eds.), *The Central Atlantic Magmatic Province: Insights from fragments of Pangea* (pp 129-149). American Geophysical Union.

Fernandes, L. B. M., Jardim de Sá, E. F., Vasconcelos, P. M. P., & Córdoba, V. C. (2020). Structural controls and $^{40}Ar/^{39}Ar$ geochronological data of basic dike swarms in the eastern domain of the Parnaíba Basin, northeast Brazil. *Journal of South American Earth Science*, *101*, 102601. https://doi.org/10.1016/j.jsames.2020.102601

Fodor, R. V., Sial, A. N., Mukasa, S. B., & McKee, E. H. (1990). Petrology, isotope characteristics, and K-Ar ages of the Maranhão, northern Brazil, Mesozoic basalt province. *Contributions to Mineralogy and Petrology*, *104*(5), 555-567.

Gill, R. (2010). Igneous rocks and processes. A practical guide. Wiley-Blackwell.

Góes, A. M. O. (1995). *A Formação Poti (Carbonífero Inferior) da Bacia do Parnaíba* [PhD Thesis, Universidade de São Paulo].

Góes, A. M. O., Travassos, W. A. S, & Nunes, K. (1993). *Projeto Parnaíba: reavaliação da bacia e perspectivas exploratórias*. Relatório Interno. Petrobras-Depex.

Harte, B. (1983). Mantle peridotites and processes: the kimberlite sample. In C. J. Hawkesworth & M. J. Norry (Eds.), *Continental Basalts and Mantle Xenoliths*, pp. 46-91. Shiva.

Hasui, Y., & Haralyi, N. L. E. (1991). Aspectos lito-estruturais e geofísicos do soerguimento do Alto Parnaíba. *Geociências*, *10*, 57-77.

Hawkesworth, C. J., Gallagher, S., Mantovani, M., Peate, D. W., Regelous, M., & Rogers, N. W. (1992). Parana magmatism and the opening of the South Atlantic. In B. C. Storey, C. Alabaster & R. J. Pankhurst (Eds.), *Magmatism and the causes of continental break-up* (Vol. 68, pp. 221-240). Geological Society Special Publications. https://doi.org/10.1144/GSL.SP.1992.068.01.14

Heilbron, M., Guedes, E., Mane, M., Valeriano, C. M., Tupinambá, M., Almeida, J., Eirado Silva, L. G., Duarte, B. P., Della Favera, J. C., & Viana, A. (2018). Geochemical and temporal provinciality of the magmatism of the eastern Parnaíba Basin, NE Brazil. In M. C. Daly, R. A. Fuck, J. Julià, D. I. M. Macdonald & A. B. Watts (Eds.), *Cratonic basin formation: a case study of the Parnaíba Basin of Brazil* (Vol. 472, pp. 251-278). Geological Society. https://doi.org/10.1144/SP472.11

Heimdal, T., Jones, M. T., & Svensen, H. H. (2020). Thermogenic carbon release from the Central Atlantic magmatic province caused major end-Triassic carbon cycle perturbation. *PNAS*, *117*(22), 11968-11974. https://doi.org/10.1073/pnas.2000095117

Hémond, C., Hofmann, A. W., Vlastélic, I., & Nauret, F. (2006). Origin of MORB enrichment andrelative trace element compatibilities along the Mid-Atlantic Ridge between 10o and 24oN. Geochem. Geophys. Geosyst, 7(12), 1-22. https://doi.org/10.1029/2006GC001317

Hergt, J. M., Peate, D. W., & Hawkesworth, C. J. (1991). The petrogenesis of Mesozoic Gondwana low-Ti flood basalts. *Earth and Planetary Science Letters*, *105*(1-3), 134-148. https://doi.org/10.1016/0012-821X(91)90126-3

Hoernle, K., Rohde, J., Hauff, F., Garbe-Schönberg, D., Homrighausen, S., Werner, R., & Morgan, J. P. (2015). How and when plume zonation appeared during the 132 Myr evolution of the Tristan Hotspot. *Nature Communications*, *6*, 7799. https://doi.org/10.1038/ncomms8799

Hollanda, M. H. B., Archanjo, C. J., Macedo Filho, H., Fossen, R. E., Ernst, R. E., De Castro, D. L., Melo, A. C., & Oliveira, A. L. (2019). The Mesozoic Equatorial Atlantic Magmatic Province (EQUAMP): a new large igneous province in South America. In R. K. Srivastava, R. E. Ernst & P. Peng (Eds.), *Dyke swarms of the world: a modern perspective* (pp. 87-110). Springer Geology.

Irvine, T. N., & Baragar, W. R. A. (1971). A guide to the chemical classification of the common volcanic rocks. *Canadian Journal of Earth Science*, *8*(5), 523-548. https://doi.org/10.1139/e71-055

Ivanov, A. V., Demonterova, E. I., Rasskazov, S. V., & Yasnygina, T. A. (2008). Low-Ti melts from the southeastern Siberian Traps Large Igneous Province: evidence for a water-rich mantle source? *Journal of Earth System Science*, *117*(1), 1-21. https://doi.org/10.1007/s12040-008-0008-z

King, S. D., & Anderson, D. L. (1995). An alternative mechanism to flood basalt formation. *Earth and Planetary Science Letters*, *136*(3-4), 269-279. https://doi.org/10.1016/0012-821X(95)00205-Q

Le Bas, M. J., Le Maitre, R. W., Streckeisen, A., & Zanettin, B. (1986). A chemical classification of volcanic rocks based on the total alkali–silica diagram. *Journal of Petrology*, *27*(3), 745-750. https://doi.org/10.1093/petrology/27.3.745

Leite, J. F., Aboarrage, A. M., & Daemon, R. F. (1975). *Projeto Carvão da Bacia do Parnaíba: relatório final das etapas II e III* (Vol. 1). Departamento Nacional de Pesquisa Mineral/ Companhia de Pesquisas de Recursos Minerais.

Lima, E. A., & Leite, J. F. (1977). *Projeto estudo global dos recursos minerais da Bacia Sedimentar do Parnaiba: integração geologico-metalogenetica: relatório final da etapa III*. CPRM.

Lustrino, M. (2005). How the delamination and detachment of lower crust can influence basaltic magmatism, *Earth-Science Reviews*, *72*(1-2), 21-38. https://doi.org/10.1016/j.earscirev.2005.03.004

Luttinen, A. V., Heinonen, J. S., Kurhila, M., Jourdan, F., Mänttäri, I., Vuor, S. K., & Huhma, H. (2015). Depleted Mantle-sourced CFB Magmatism in the Jurassic Africa–Antarctica Rift: Petrology and 40Ar/39Ar and U/Pb Chronology of the Vestfjella Dyke Swarm, Dronning Maud Land, Antarctica. *Journal of Petrology*, *56*, 919-952. https://doi.org/10.1093/petrology/egv022

Macedo Filho, A. A., Hollanda, M. H. B. M., Archanjo, C. J., Ávila, C. F., & Oliveira A. L. (2023a). Unraveling the tectonic setting and crystallization history of the Equatorial Atlantic Magmatic Province. *Tectonophysics*, *858*, 229881. https://doi.org/10.1016/j.tecto.2023.229881

Macedo Filho, A. A., Hollanda, M. H. B. M., Oliveira, A. L., & Negri, F. A. (2023b). Magma plumbing systems in the Parnaíba Basin: Geochemistry, geochronology, and regional correlations with Mesozoic large igneous provinces. *Lithos*, *446-447*, 107130. https://doi.org/10.1016/j.lithos.2023.107130

Machado, F. B., Rocha-Junior, E. R. V., Marques, L. S., & Nardi, A. J. R. (2015). Volcanological aspects of the northwest region of Paraná continental flood basalts (Brazil). *Solid Earth*, *6*(1), 227-241. https://doi.org/10.5194/se-6-227-2015

Magalhães, Y. V. (2019). *Petrologia dos diabásios da região de Piripiri-PI, Bacia do Parnaíba* [Monography, Universidade Federal Rural do Rio de Janeiro].

Mahoney, J. J., Sheth, H. C., Chandrasekharam, D., & Peng, Z. X. (2000). Geochemistry of Flood Basalts of the Toranmal Section, Northern Deccan Traps, India: Implications for Regional Deccan Stratigraphy. *Journal of Petrology*, *41*(7), 1099-1120. https://doi.org/10.1093/petrology/41.7.1099

Marsh, J. (1987). Basalt geochemistry and tectonic discrimination within continental flood basalt provinces. *Journal of Volcanology and Geothermal Research*, *32*, 35-49.

Marzoli, A., Callegaro, S., Dal Corso, J., Davies, J. F. L., Chiaradia, M., Youbi, N., Bertrand, H., Reiberg, L., Merle, R., & Jourdan, F. (2018). The Central Atlantic Magmatic Province (CAMP): a review. In L. H. Tanner (Ed.). *The Late Triassic World, Topics in Geobiology 46*.

Marzoli, A., Jourdan, F., Puffer, J. H., Cuppone, T., Tanner, L. H., Weems, R. E., Bertrand, H., Cirilli, S., Bellieni, G., & De Min, A. (2011). Timing and duration of the Central Atlantic magmatic province in the Newark and Culpeper basins, eastern USA. *Lithos*, *122*(3-4), 175-188. https://doi.org/10.1016/j.lithos.2010.12.013

Marzoli, A., Renne, P. R., Piccirillo, E. M., Ernesto, M., Bellieni, G., & De Min, A. (1999). Extensive 200-millionyear-old continental flood basalts of the Central Atlantic Magmatic Province. *Science*, *284*(5414), 616-618. https://doi.org/10.1126/science.284.5414.616

McDonough, W. F., & Sun, S. S. (1995). The composition of the earth. *Chemical Geology*, *120*(3-4), 223-253. https://doi.org/10.1016/0009-2541(94)00140-4

McHone, J. G. (2000). Non-plume magmatism and rifting during the opening of the central Atlantic Ocean. *Tectonophysics*, *316*(3-4), 287-296. https://doi.org/10.1016/S0040-1951(99)00260-7

Merle, R., Marzoli, A., Bertrand, H., Reisberg, L., Verat, I. C., Zimmermann, C., Chiaradia, M., Belienni, G., & Ernesto, M. (2011). $^{40}Ar/^{39}Ar$ ages and Sr-Nd-Pb-Os geochemistry of CAMP tholeiites from Western Maranhão basin (NE Brazil). *Lithos*, *122*(3-4), 137-151. https://doi.org/10.1016/j.lithos.2010.12.010

Merle, R., Marzoli, A., Reisberg, L., Bértrand, H., Nenchim, A., Chiaradia, M., Callegaro, S., Jourdan, F., Belienni, G., Konttak, D., Puffer, J., & McHone, J. C. (2014). Sr, Nd, Pb and Os Isotope Systematics of CAMP Tholeiites from Eastern North America (ENA): Evidence of a Subduction-enriched Mantle Source. *Journal of Petrology*, *55*(1), 133-180. https://doi.org/10.1093/petrology/egt063

Milani, E. J., & Thomaz Filho, A. (2000). Sedimentary basins of South America. In: *Tectonic Evolution of South America* (pp. 389-452). 31th International Geological Congress.

Miloski, P., Mendes, J. C., Almeida, C. N., Valente, S. C., & Medeiros, S. R. (2019). Petrogenesis of Continental Flood Basalts in eastern Parnaíba basin, Brazil: a singular sill occurrence with Low- and High-Ti tholeiites. *Journal of South American Earth Sciences*, *94*, 102192. https://doi.org/10.1016/j.jsames.2019.05.008

Mocitaiba, L. S. R., De Castro, D. L., & Oliveira, D. C. (2017). Cartografia geofísica regional do magmatismo mesozoico na Bacia do Parnaíba. *Geologia USP Série Científica*, *17*(2), 169-192. https://doi.org/10.11606/issn.2316-9095.v17-455

Oliveira, A. L., Pimentel, M. M., Fuck, R. A., & Oliveira, D. C. (2018). Petrology of Jurassic and Cretaceous basaltic formations from the Parnaíba Basin, NE Brazil: correlations and associations with large igneous provinces. In M. C. Daly, R. A. Fuck, J. Juliá, D. I. M. MacDonald & A. Watts (Eds.), *Cratonic Basin Formation: a case study of the Parnaíba Basin of Brazil* (pp. 472). Geological Society.

Pearce, J. A. (1982). Trace element characteristics of lavas from destructive plate boundaries. In R. S. Thorpe (Ed.), *Andesites* (pp. 525-548). Wiley.

Pearce, J. A., & Norry, M. J. (1979). Petrogenetic implications of Ti, Zr, Y and Nb variations in volcanic rocks. *Contributions to Mineralogy and Petrology*, *69*, 33-47. https://doi.org/10.1007/BF00375192

Pearce, J. A., Ernst, R. E., Peate, D. W., & Rogers, D. (2021). LIP printing: Use of immobile element proxies to characterize Large Igneous Provinces in the geologic record. *Lithos*, *392-393*, 106068. https://doi.org/10.1016/j.lithos.2021.106068

Peate, D. W. (1997). The Parana-Etendeka Province. In J. J. Mahoney & M. F. Coffin (Eds.), *Large igneous provinces: continental, oceanic, and planetary flood volcanism* (Vol. 100, pp. 217-245). American Geophysical Union.

Peate, D. W., & Hawkesworth, C. J. (1996). Lithospheric to asthenospheric transition in Low-Ti flood basalts from southern Paraná, Brazil. *Chemical Geology*, *127*(1-3), l-24. https://doi.org/10.1016/0009-2541(95)00086-0

Peate, D. W., Hawkesworth, C. J., & Mantovani, M. S. M. (1992). Chemical stratigraphy of the Paraná lavas (South America): classification of magma types and their spatial distribution. *Bulletin of Volcanology*, *55*(1-2), 119-139. https://doi.org/10.1007/bf00301125

Peate, D. W., Mantovani, M. S. M., & Hawkesworth, C. J. (1988). Geochemical stratigraphic of the Paraná Continental Flood Basalts: borehole evidences. *Revista Brasileira de Geociências*, *18*(2), 212-221. https://doi.org/10.25249/0375-7536.19988212221

Piccirillo, E. M., & Cox, K. G. (1988). Origins of variation in the mafic rocks of the S. Parana basin. International Conference on Geochemical Evolution of the Continental Crust, pp. 83-89.

Piccirillo, E. M., Comin-Chiaramonti, P., Bellieni, G., Civetta, L., Marques, L. S., Melfi, A. J., Petrini, R., Raposo, M. I. B, & Stolfa, D. (1988). Petrogenetic aspects of continental flood basalt-rhyolite suites from the Paraná basin (Brazil). In E. M. Piccirillo & A. J. Melfi (Eds.), *The Mesozoic Flood Volcanism and the Paraná Basin*. Petrogenetic and Geophysical Aspects. Universidade de São Paulo.

Ragland, P. C. (1989). *Basic analytical petrology*. Oxford University Press.

Riley, T. R., Leat, P.T ., Curtis, M., Milan, I. L., Duncan, R. A., & Fazel, A. (2005). Early–Middle Jurassic dolerite dykes from Western Dronning Maud Land (Antarctica): identifying mantle sources in the Karoo Large Igneous Province. *Journal of Petrolugy*, *46*(7), 1489-1524. https://doi.org/10.1093/petrology/egi023

Rocha-Junior, E. R. V., Marques, L. S., Babinski, M., Nardi, A. J. R., Figueiredo, A. M. G., & Machado, F. B. (2013). Sr, Nd, Pb isotopic constraints on the nature of the mantle sources involved in the genesis of the high-Ti tholeiites from northern Paraná Continental Flood Basalts (Brazil). *Journal of South American Earth Sciences*, *46*, 9-25. https://doi.org/10.1016/j.jsames.2013.04.004

Rodrigues, J. B. (2014). *Relatório interno. Projeto Opala*. Brazil Geological Survey.

Ruiz-Martínez, V. C., Torsvik, T. H., van Hinsbergen, D. J. J., & Gaina, C. (2012). Earth at 200 Ma: Global palaeogeography refined from CAMP palaeomagnetic data. *Earth and Planetary Science Letters*, *331-332*, 67-79. https://doi.org/10.1016/j.epsl.2012.03.008

Schobbenhaus, C., Gonçalves, J. H., Santos, J. O. S., Abram, M. B., Leão Neto, R., Matos, G. M. M., Vidotti, R. M., Ramos, M. A. B., & Jesus, J. D. A. (2004). *Carta geológica do Brasil ao milionésimo sistema de informações geográficas*. Programa Geologia do Brasil.

Scribelk, L. S. (2019). *Petrologia dos diabásios da região de Colinas, Bacia do Parnaíba* [Monography. Universidade Federal Rural do Rio de Janeiro].

Silva, A. G., Almeida, C. N., Valente, S. C., & Borghi, L. (2017). The petrogenesis of tholeiitic microgabbro in eastern Parnaíba Basin: evidence for geochemical heterogeneities in the subcontinental lithospheric mantle in NE Brazil. *Brazilian Journal of Geology*, *47*(1), 109-126. https://doi.org/10.1590/2317-4889201720160041

Thomaz Filho, A., Misuzaki, A. M. P., & Antonioli, L. (2008). Magmatismo nas bacias sedimentares brasileiras e sua influência na geologia do petróleo. *Revista Brasileira de Geociências*, *38*(2), 128-137.

Vaz, P. T., Rezende, N. G. A. M., Wanderley Filho, J. R., & Travassos, W. A. S. (2007). Bacia do Parnaíba. *Boletim de Geociências da Petrobras*, *15*(2), 253-263.

Wang, H., van Hunen, J., & Pearson, D.H. (2015). The thinning of subcontinental lithosphere: The roles of plume impact and metasomatic weakening. *Geochemistry, Geophysics, Geosystems*, *16*(4), 1156-1171. https://doi.org/10.1002/2015GC005784

Whalen, L., Gazel, E., Vidito, C., Puffer, J., Bizimis, M., Henika, W., & Caddick, M. J. (2015). Supercontinental inheritance and its influence on supercontinental breakup: the Central Atlantic Magmatic Province and the breakup of Pangea. *Geochemistry, Geophysics, Geosystems*, *16*(10), 3532-3554. https://doi.org/10.1002/2015GC005885

Winchester, J. A., & Floyd, P. A. (1977). Geochemical discrimination of different magma series and their differentiation product using immobile elements. *Chemical Geology*, *20*, 325-343. https://doi.org/10.1016/0009-2541(77)90057-2